

Convective heat transfer past a three side-by-side square cylinders using double MRT- lattice Boltzmann method

Y. ADMI ^a, M.A. MOUSSAOUI ^a, A. MEZRHAB ^a, V. BOTTOM ^b, D. HENRY ^b

^aLaboratory of Mechanics & Energy, Faculty of Sciences, Mohammed 1st University, 60000 Oujda, Morocco.

Email : lahmerelbachir@gmail.com, moussaoui.amine@gmail.com, amezrhab@yahoo.fr

^bLaboratoire de Mécanique des Fluides et d'Acoustique, CNRS/Université de Lyon, Ecole Centrale de Lyon/Université Lyon 1/INSA de Lyon, ECL, 36 Avenue Guy de Collongue, 69134 Ecully Cedex, France

Email : valery.botton@insa-lyon, daniel.henry@ec-lyon.fr

Résumé :

Dans cet article, on étudie numériquement l'écoulement laminaire et les caractéristiques de transfert de chaleur dans un canal horizontal bidimensionnel contenant trois obstacles carrés chauffés. Le schéma numérique est basé sur la méthode de Boltzmann sur réseau avec temps multiples de relaxation (MRT-LBM). Les champs des lignes de courant et de température sont traités respectivement à l'aide des modèles MRT-D2Q9 et MRT-D2Q5. L'écoulement est considéré comme laminaire, incompressible et bidimensionnel. Le fluide circulant dans le canal est l'air ($Pr = 0,71$) et ses propriétés physiques, à l'exception de sa densité, sont supposées être constantes. Les deux parois du canal sont supposées adiabatiques, la température de l'air à l'entrée est fixée à température froide et la température de chaque cylindre est chaude. Les effets du nombre de Reynolds et des distances séparant les obstacles, sur l'écoulement du fluide et le transfert de chaleur sont examinés. Les résultats sont présentés en termes de lignes de courant et d'isothermes.

Abstract:

In the present paper, a numerical simulation is performed to study the laminar flow and the heat transfer characteristics in a two-dimensional horizontal channel containing three heated square obstacles (blocks) placed side-by-side unequally or equally spaced. The numerical scheme is based on a Double Multiple Relaxation Time Lattice Boltzmann Method (MRT-LBM). The flow and the temperature fields are treated using the MRT-D2Q9 model and the MRT-D2Q5 model, respectively. The problem considered here is laminar, incompressible, and two-dimensional flow. The fluid circulating in the channel is the air ($Pr = 0.71$) and its physical properties, except its density, are supposed to be constant. The two channel walls are assumed to be adiabatic, the temperature of the incoming air flow is fixed at cold temperature, and the temperature of each cylinder is hot. Effects of the Reynolds number and the dimensionless separation distances $a1$ and $a2$ on the fluid flow and the heat transfer, are examined. The simulation results are presented in terms of streamline contours and isotherms.

Mots clefs: Lattice Boltzmann method (LBM), the heat transfer characteristics, square obstacles, Double Multiple Relaxation Time Lattice Boltzmann Method (MRT-LBM).

1 Introduction

In the last few years, the research of fluid flow and heat transfer in channels earn a great attention by the scientific community in several areas of engineering applications, such as electronic equipment cooling, heat transfer enhancement, heat exchanger, and many others industrial engineering problems [1]. To model this kind of engineering applications, the Lattice Boltzmann Method (LBM), derived from Lattice Gas Automata (LGA), is more and more adopted to solve complex problems related to fluid dynamics and thermal transfer with complex geometries [2]. The main reason of using this alternative method is the simplicity and accuracy of the simulation code. It also provides satisfactory results when solving the physical problems of fluid flow and heat transfer.

In this paper, A double multiple relaxation time (DMRT) thermal lattice Boltzmann method is applied in two-dimensional horizontal channel containing obstacles. Considering these advantages in comparison to other methods, this relatively recent method is widely used [1-7]. Alamyane and Mohamad [4] employed the double-populations LBM-BGK approach to solve the forced convection in a channel with extended surfaces mounted in the lower wall. Moussaoui et al. [5] successfully applied the Hybrid thermal lattice Boltzmann method (HTLBM) to study the fluid flow and heat transfer in an obstructed channel. Mezhhab et al. [6] conducted a numerical simulation to study the natural convection in cavity using the double MRT thermal LBM. Breuer et al. [7] performed precise calculations of laminar flow past a square cylinder using two different methods (LBM and FVM). Alam and Zhou [8] have studied the wake structure mechanism experimentally for two side-by-side cylinders by fixed Re at 300 and varying the distance between obstacles from 1 to 5. Abbasi et al. [9] numerically studied the effect of Re for flow beyond an aligned square configuration and observed different flow patterns. Islam et al. [10] numerically studied the WSM and hydrodynamic forces of flow over three SBS square cylinders using the multi-relaxation time lattice Boltzmann method (MRT-LBM). They investigated the effect of equal and unequal g between the cylinders and visualized four distinct flow regimes (asymmetric, antiphase modulated synchronized, bi-stable and modulated synchronized) at $Re = 150$. Mizushima and Akinaga. [12] discussed the numerical investigation of wakes interaction formed over a row of square cylinders. Djenidi [13] used the LBM for numerical simulation to investigate the grid generated turbulence for grids made of floating square elements. Gal et al. [14], Islam et al. [15] examined the influence of spacing distance of flow past five SBS rectangular cylinders at fixed $Re = 150$. as well as others, but all these researchers' or these authors' found that the behaviour of flow is steady. Although, this stability will disappear for the large Reynolds numbers. The recirculations produced give rise to undulations and vortex along the canal.

The main purpose of this work is to study laminar flow and heat transfer characteristics in a two-dimensional horizontal channel containing three heated square obstacles. The numerical parametric studied are: the Reynolds number and the separation distance.

2 Description of the problem and numerical method

2.1 Description of the problem:

The physical problem studied concerns a laminar flow in a two-dimensional horizontal channel containing three heated square obstacles (blocks) placed side-by-side vertically of

width d , and spaced from a dimensionless distance a_1 and a_2 , as illustrated in Fig. 1. The blockage ratio is fixed to $B=1/8$. In order to reduce the influence of the input and output boundary conditions, the channel length is set to $L = 50d$. The heat transfer fluid considered in this study is air ($Pr = 0.71$) and its physical properties, with the exception of its density, are assumed to be constant. The cylinders are placed at a distance X_{in} downstream of the inlet section of the channel. The two walls of the channel are assumed adiabatic, the temperature of the incoming airflow is fixed at $\theta_c = -0.5$ (cold temperature) and the temperature of each cylinder is constant and equal to $\theta_h = 0.5$ (hot temperature). At the inlet, the flow is fully developed with a parabolic velocity profile and as well as at the outlet, the temperature and velocity gradients are assumed to be zero.

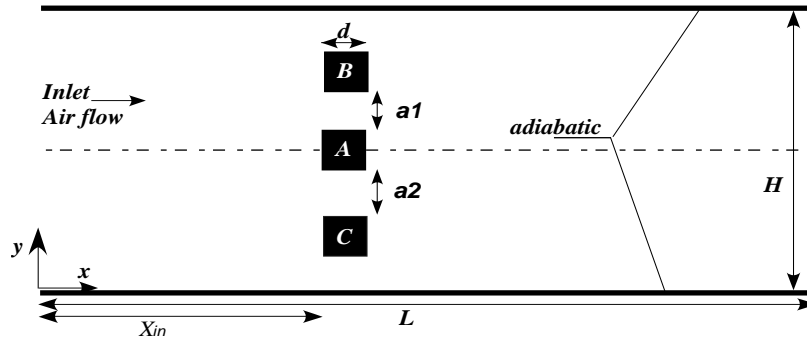


Fig.1. The physical configuration studied

2.1 The description of numerical method

The numerical scheme is based on a Double Multiple Relaxation Time Lattice Boltzmann Method (MRT-LBM). This new and innovative method based on the development of statistical physics and the appearance of cellular automata is characterized by its simplicity, precision and efficiency for the direct numerical simulation of hydrodynamic phenomena in complex geometries [2]. The flow and the temperature fields are treated using respectively the MRT-D2Q9 model and the MRT-D2Q5 model [2, 16].

2.1.1. MRT-D2Q9 model

In this approach, the fluid domain is discretized by a group of microscopic particles. The density distributions of these particles perform two types of motions: collision and diffusion. Figure 2 illustrates the numerical scheme of the D2Q9 model used (where D corresponds to the dimensions of the space and Q to the number of particles of a computing node). This square grid is spaced uniformly ($\partial x = \partial y$). The use of the MRT model (multi-relaxation time) introduced by Humières [17]. It has been clearly demonstrated that the lattice Boltzmann Equation (LBE) models with collision operators with TRMs have inherent advantages over their BGK counterparts which is the Bhatnagar - Gross - Krook (BGK) equation based on an approximation of the simple relaxation time, for example [18, 19]. MRT-LBE models are much more stable than BGK because the different relaxation times can be adjusted individually to achieve "optimal" stability [20].

The fluid particles move from one node of the grille to an adjacent node with discrete speeds that are given by:

$$c_i \begin{cases} (0, 0); & i = 0 \\ (\cos[(i-1)\pi/2], \sin[(i-1)\pi/2])c; & i = 1 - 4 \\ (\cos[(2i-9)\pi/4], \sin[(2i-9)\pi/4])c; & i = 5 - 8 \end{cases} \quad (1)$$

The MRT-LBM can be written as follows:

$$f_i(x + c_i \Delta t, t + \Delta t) = f_i(x, t) + \Omega f_i(x, t), \quad i = 0, 1, \dots, 8 \quad (2)$$

Where f_i is distribution function of a particle and Ω is the collision operator representing the variation of the distribution function due to collisions between particles.

The collision step in the speed space is difficult to be performed. It is more practical to perform the collision process in the momentum space [21]. The previous equation becomes:

$$f_i(x + c_i \Delta t, t + \Delta t) = f_i(x, t) - M^{-1}S[m(x, t) - m^{eq}(x, t)] \quad i = 0, 1, \dots, 8 \quad (3)$$

Where m and m^{eq} represent the moment vectors and S the diagonal relaxation matrix. The passage from the space of the velocities to the space of the quantities of motions can be carried out by the following linear transformation: $m = Mf$ and $f = M^{-1}m$. Where the matrix M of order 9 is given by [21] :

$$M = \begin{pmatrix} \langle m_0 | \\ \langle m_1 | \\ \langle m_2 | \\ \langle m_3 | \\ \langle m_4 | \\ \langle m_5 | \\ \langle m_6 | \\ \langle m_7 | \\ \langle m_8 | \end{pmatrix} = \begin{pmatrix} 1 & 1 & 1 & 1 & 1 & 1 & 1 & 1 & 1 \\ 0 & 1 & 0 & -1 & 0 & 1 & -1 & -1 & 1 \\ 0 & 0 & 1 & 0 & -1 & 1 & 1 & -1 & -1 \\ -4 & -1 & -1 & -1 & -1 & 2 & 2 & 2 & 2 \\ 4 & -2 & -2 & -2 & -2 & 1 & 1 & 1 & 1 \\ 0 & -2 & 0 & 2 & 0 & 1 & -1 & -1 & 1 \\ 0 & 0 & -2 & 0 & 2 & 1 & 1 & -1 & -1 \\ 0 & 1 & -1 & 1 & -1 & 0 & 0 & 0 & 0 \\ 0 & 0 & 0 & 0 & 0 & 1 & -1 & 1 & -1 \end{pmatrix} \quad (4)$$

The moment vector m is:

$$m = (m_0, m_1, m_2, \dots, m_8)^T \quad (5)$$

The choice of the equilibrium functions m_i^{eq} will determine the equivalent macroscopic equations.

$$\begin{aligned} m_0^{eq} &= \rho \\ m_1^{eq} &= j_x \\ m_2^{eq} &= j_y \\ m_3^{eq} &= -2\rho + 3(j_x^2 + j_y^2) \\ m_4^{eq} &= \rho - 3(j_x^2 + j_y^2) \\ m_5^{eq} &= -j_x \\ m_6^{eq} &= -j_y \\ m_7^{eq} &= (j_x^2 - j_y^2) \\ m_8^{eq} &= j_x j_y \end{aligned} \quad (6)$$

Where

$$j_x = \rho u_x = \sum_i f_i^{eq} c_{ix} \quad (7)$$

$$j_y = \rho u_y = \sum_i f_i^{eq} c_{iy}. \quad (8)$$

It is important to note that during the collision step, which is local in space, three moments are preserved (the density and the momentum). The other six remaining, non-conserved moments are calculated from a simple linear relaxation equation to the equilibrium values that depend on the conserved quantities [22].

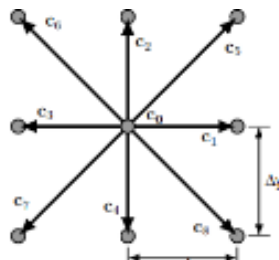


Fig.2. The Lattice structure for the D2Q9 model

The diagonal matrix S is giving by:

$$S = \text{diag} (1.0, 1.4, 1.4, s_3, 1.2, s_5, 1.2, s_7, s_8) \quad (9)$$

Where $s_7 = s_8 = \frac{2}{(1+6\nu)}$, s_3 and s_5 are arbitrary (in our case, $s_3=s_4=1.0$).

The distribution function of the local equilibrium can be given by:

$$f_i^{eq} = \rho w_i \left[1 + \frac{3}{c^2} c_i + \frac{9}{2c^4} (c_i \cdot \mathbf{u})^2 - \frac{3}{2c^2} \mathbf{u} \cdot \mathbf{u} \right] \quad i = 0, 1, \dots, 8 \quad (10)$$

Where $w_0 = 4/9$, $w_i = 1/9$ ($i = 1, 2, 3, 4$), $w_i = 4/9$ ($i = 5, 6, 7, 8$)

The macroscopic quantities such as: the density of the masse ρ and the velocity \mathbf{u} are given by the summations of the distribution function

$$\rho = \sum_{i=0}^8 f_i, \quad \rho \mathbf{u} = \sum_{i=0}^8 c_i f_i \quad (11)$$

2.1.2. MRT-D2Q5 model

In this study, the advection diffusion equation of temperature has been solved by a second function of distributions g_i whose evolution is also described by the MRT-LBM. For the reason of simplicity, it is preferable to use a spaced square D2Q5 network $\partial x = \partial y$ illustrated in (Figure3).

In this model (D2Q5) the fluid particles move from one node of the grid to an adjacent node with discrete velocities which are given by:

$$c_i \begin{cases} (0, 0); & i = 0 \\ (\cos[(i-1)\pi/2], \sin[(i-1)\pi/2])c; & i = 1-4 \end{cases} \quad (12)$$

The function of discrete distributions g_i (MRT-LBE can be expressed as [22]:

$$g_i(\mathbf{x} + c_i \Delta t, t + \Delta t) = g_i(\mathbf{x}, t), \quad i = 1, 2, 3, 4 \quad (13)$$

In the same way as the functions of distributions f_i , there are two fundamental steps for particle motion: the collision step and the advection step. The collision process is difficult to be achieved in the speed space, as indicated in ref. [23].

Practically, this process is realized in the space of moments. This is why, we define (m_k) moments based on the distribution (g_j) on the basis of the following linear transformation:

$$m_k = \sum_{j=0}^4 M_{kj} g_j, \quad 0 \leq k \leq 4$$

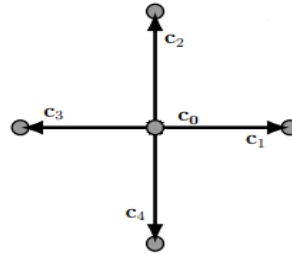


Fig. 3. The Lattice structure for the D2Q5 model

For this model, the transformation matrix M can be expressed as follows:

$$M = \begin{pmatrix} 1 & 1 & 1 & 1 & 1 \\ 0 & 1 & 0 & -1 & 0 \\ 0 & 0 & 1 & 0 & -1 \\ -4 & 1 & 1 & 1 & 1 \\ 0 & 1 & -1 & 1 & -1 \end{pmatrix} \quad (14)$$

Note that the matrix M is invertible and orthogonal.

To simulate the diffusion problems, we keep only the first moment of the collision stage and we obtain the following expression:

$$m_0 = T = \sum_{j=0}^4 g_j \quad (15)$$

For non-conserved moments, we assume that they relax to the equilibrium m_k^{eq} which are non-linear functions of conserved quantities and are defined by the following relation:

$$m_k = (1 - s_k)m_k + s_k m_k^{eq}, \quad 1 \leq k \leq 4 \quad (16)$$

Where $s_k = \delta t / \tau_k$ is the relaxation ratio that satisfies the constraint $0.5 \leq s_k \leq 2$ to get a stable numerical scheme. The relaxation ratios s_k are not identical as in the case of the so-called BGK method. In our work we choose :

$$m_0^{eq} = T, m_1^{eq} = uT, m_2^{eq} = vT, m_3^{eq} = aT \text{ et } m_4^{eq} = 0. \quad (17)$$

Where (a) is a constant related to thermal diffusivity by the following relation: $\alpha = \frac{\sqrt{3}(4+a)}{60}$

The advection-diffusion equation described by the LBM model is:

$$\frac{\delta T}{\delta t} + u \nabla T - \alpha \left(\frac{\delta^2 T}{\delta x^2} + \frac{\delta^2 T}{\delta y^2} \right) = O(\delta t^2) \quad (18)$$

With $s = \frac{1}{5\alpha} + 0.5$ where $\alpha = \left(\frac{1}{s} - \frac{1}{2}\right)/5$ represents the diffusion factor.

3. Boundary conditions

In LBM simulations, implementing boundary conditions occupy a big importance. In fact, the unknown distribution functions pointing to the fluid zone at the boundary nodes must be known. For the walls, the most widely used conditions are based on rebound method [24]. In our simulations, we applied this type of conditions to know the boundary conditions of the obstacles. It should be noted that the two walls of the channel are supposed to be adiabatic, that is why we have used adiabatic boundary conditions for the lower and upper wall of the canal. While at the entrance, the flow is fully developed with a parabolic velocity profile, so we have implemented boundary conditions of Zou and He [25]. The distribution function g can be obtained as follows:

$$g_j = \sum_{k=0}^4 (M^{-1})_{jk} m_k \quad \text{et} \quad g_1 + g_3 = 2T \left(1 + \frac{a}{4}\right) / 5 \quad (19)$$

Where M^{-1} is the inverse matrix of moment and a is calculated by the preceding formula

$$\alpha = \frac{\sqrt{3}(4+a)}{60}.$$

This condition $g_1 = -g_3 + 2\theta_c \left(1 + \frac{a}{4}\right) / 5$ is applied in inlet of channel as well as to the channel input. Whereas for the obstacle limits, we use the same condition, replacing θ_c with θ_h because the limits of the obstacles are considered hot. Then, adding the condition $g_2 = -g_4 + 2\theta_c \left(1 + \frac{a}{4}\right) / 5$. For the lower and upper faces of obstacles.

Similarly, for the thermal boundary conditions, we used the adiabatic conditions for the canal walls.

4. Validation:

As discussed in the introduction, the flow problem around a square cylinder is a thematic research topic and is treated by several researchers such as Davis et al. [26]; Bernsdorf et al.

[27]; Breuer et al. [7]; Moussaoui et al. [5] and others. We compare our results to those presented by Breuer et al. [7]. We consider a confined flow around a square-section cylinder mounted inside a flat channel with a 1/8 blockage ratio. Two parameters are validated: The recirculation curve as a function of the Reynolds number and the velocity curves.

The recirculation length is one of the most important parameters for flows around obstacles. Fig. 4 shows that the variation of recirculation lengths with respect to the diameter of the obstacle as a function of the Reynolds number is almost linear. The curve on the right represents our results obtained from LBM and the curve on the left represents the results obtained by Breuer et al. [7]. As can be seen, our results are generally in good agreement with those of Breuer et al. [7]. The small differences between the two results can be due to the mesh used or the thermal effects processed in our simulation.

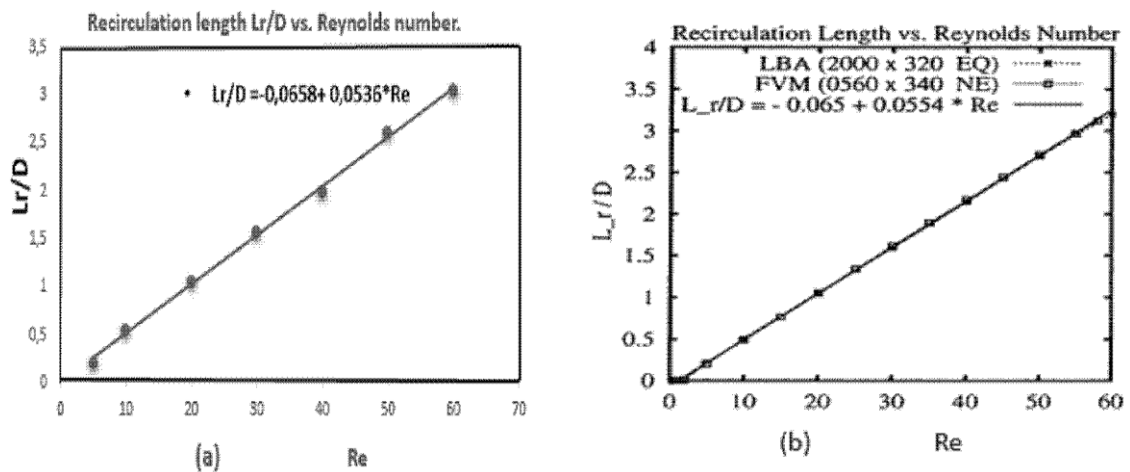


Fig. 4. Computed recirculation length L_r vs Reynolds number: (a) Our result, (b): Reference

Let us note a linear dependence between the length of the recirculations and the Reynolds number. This is expressed by the following linear equation:

$$L_r/D = -0.608 + 0.0536 * Re \quad (20)$$

The recirculations lengths become increase with increasing the Reynolds number Re .

The velocity profile U obtained by our code is in good agreement with that presented by Breuer et al. [7] as shown in Figure 5. Similarly, the velocity profile (V) is compatible with reference result (fig 6):

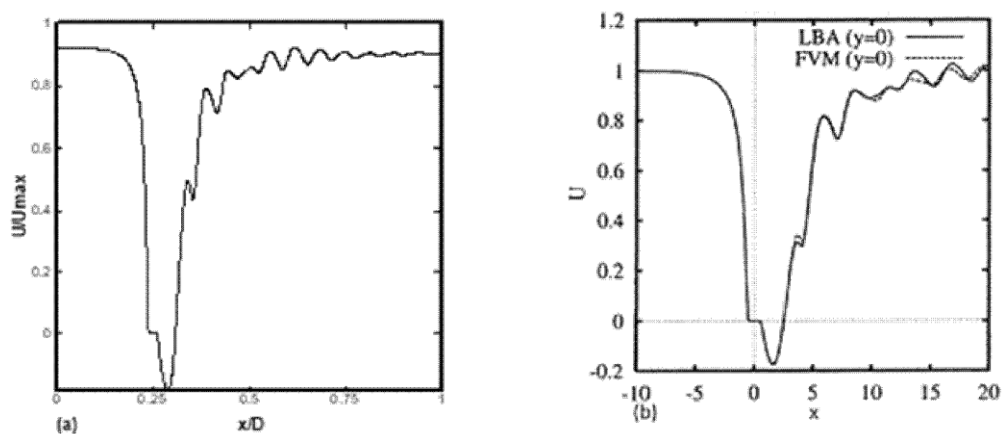


Fig.5. Comparison of velocity profile (U): (a) Present work, (b): Reference

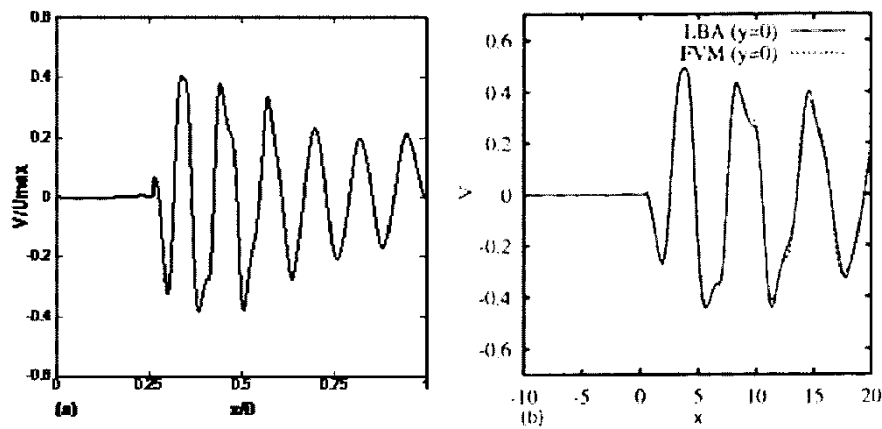


Fig.6. Comparison of velocity profile (V): (a) Present work, (b): Reference

5. Results and discussions

Numerical calculations were carried out for flow around three side-by-side square cylinders unequally or equally spaced. A Reynolds number range $20 < Re < 200$ was investigated numerically. This number is based on the cylinder diameter D and the maximum flow velocity U_{max} of the parabolic inlet profile. The next section begins with a description of the different flow and temperature fields patterns observed with varying of Re . This shows the remarkable effect of the Re on the streamlines and isothermals lines (see figures 7&8). Then, a study of the effect of dimensionless distances a_1 and a_2 separating the blocks is performed. To analyze the effect of unequal and equal spacing on the nature of flow as well as on the heat transfer characteristics, a variety of cases has been studied. In fact, in this work, four cases are analyzed (see Figures 9 & 10). We can easily observe the dynamics of the flow behind the cylinders and changes in the vortex shedding pattern. Figures 9 & 10 clearly show that the swirl vortex undergoes a significant change behind the three cylinders. It is observed in both Figures that when a_1 and a_2 are slightly increased, the vortex excretion changes completely behind the cylinders and the flow deflection changes its amplitude from one case to another.

5.1 Effect of Reynolds number

In this study, the Reynolds number is considered as the main parameter. Fig. 7 shows computational results in the vicinity of the cylinder by streamlines and isotherms for four different Reynolds numbers ($Re = 20; 60; 100; 200$) characterizing a totally different flow regime. The obtained results show that the flow is stable, permanent for low values of the Reynolds number ($Re \leq 20$). Fig. 7.a presents the streamlines for $Re = 20$. As can be seen, the flow is perfectly symmetrical. A detachment then a reattachment of the flow appeared just downstream of the cylinder.

For large Reynolds number values, the intensity of the viscous forces decreases. The symmetry obtained before disappears and the regime becomes variable in time. This instability gives rise to the formation of a wave, formed by oscillations of the flow behind the cylinder, which propagates in the direction of flow and loses its amplitude while moving away from the cylinder.

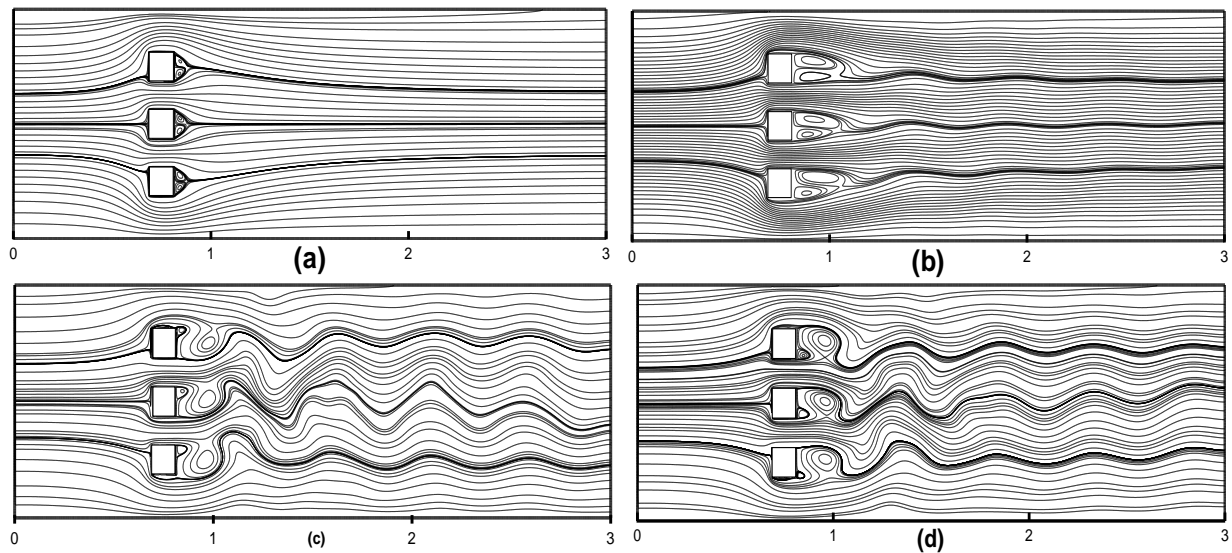


Fig.7. Streamlines around the square obstacles of different Reynolds number: (a) $Re=20$; (b) $Re=60$; (c) $Re=100$; (d) $Re=200$.

In order to determine the transition between the symmetric permanent flow and the periodic flow, a series of calculations was performed by slowly varying the value of the Reynolds number. This one appears for a critical Reynolds number close to 60. These ripples clearly manifests itself for a higher number of Reynolds (see the cases where $Re = 100$ and $Re = 200$) where we see disturbances and long recirculation's behind the cylinders.

Similarly, the temperature contours are also perfectly symmetrical and stable in time (Fig.8) for low Reynolds numbers. They are elongated in the direction of flow more flattened in the recirculation zone. However, they are unstable and asymmetric for higher Reynolds numbers.

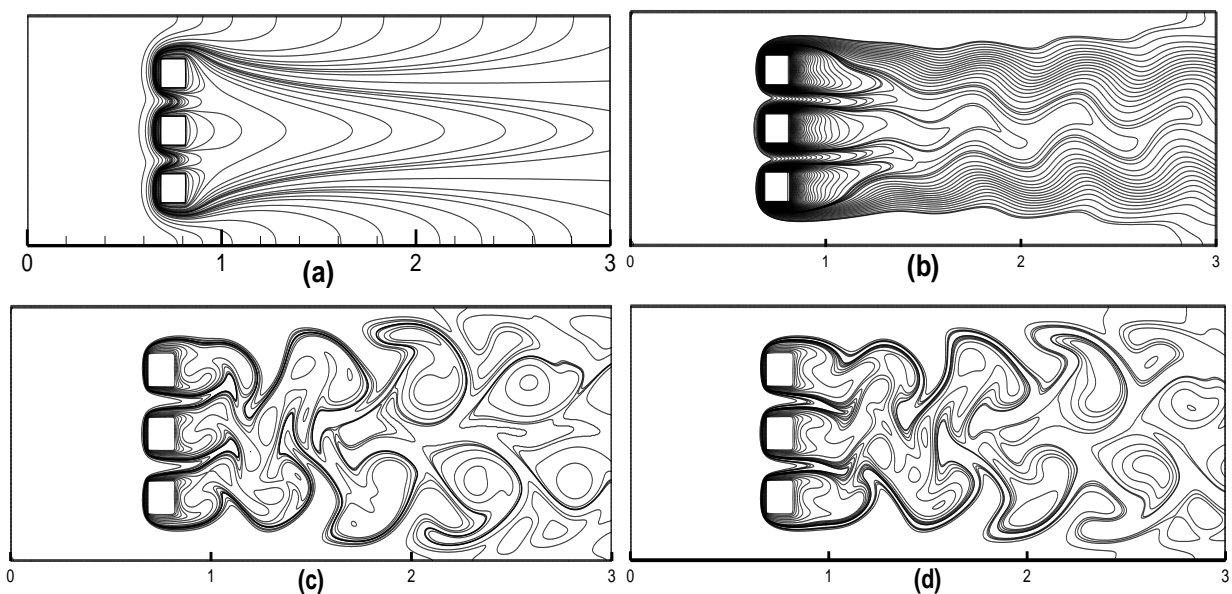


Fig.8. Isothermal lines around the square obstacles of different Reynolds number: (a) $Re=20$; (b) $Re=60$; (c) $Re=100$; (d) $Re=200$.

5.2 The effect of separation distance

To clearly observe the effect of the distance separating the obstacles, all the results included in this document are taken for a fixed Reynolds number ($Re = 100$). Four cases are discussed in this work, first, the case where $a_1 = a_2 = d$ (fig (a)), a recirculation occurs just after each obstacle, this recirculation causes undulations along the flow which shows the instability of this flow; however, it is always symmetrical. In the second case, where $a_1 > a_2$ (fig (b)) a single recirculation is produced behind the centered obstacle, while we see two recirculation produced behind each of the other obstacles. These generate a remarkable disturbance after these recirculation's, which produces two other recirculation on the lower wall. The third case discussed is similar to the first case, we only increase the separation distance, that is, $a_1 = a_2 = 2 \times d$ (fig (c)), where the obstacles are close to the wall, in this case, we see a recirculation just after each obstacle, while others are generated on the bottom wall and one on the top wall. Nevertheless, the flow regime remains almost symmetrical or quasi-symmetrical. In the last case (fig (d)), we have attached the three obstacles in order to obtain a vertical rectangle ($3 \times d$). This attachment produces a recirculation behind the rectangle and causes strong ripples along the flow, which gives rise to other recirculations on the two wall of the channel.

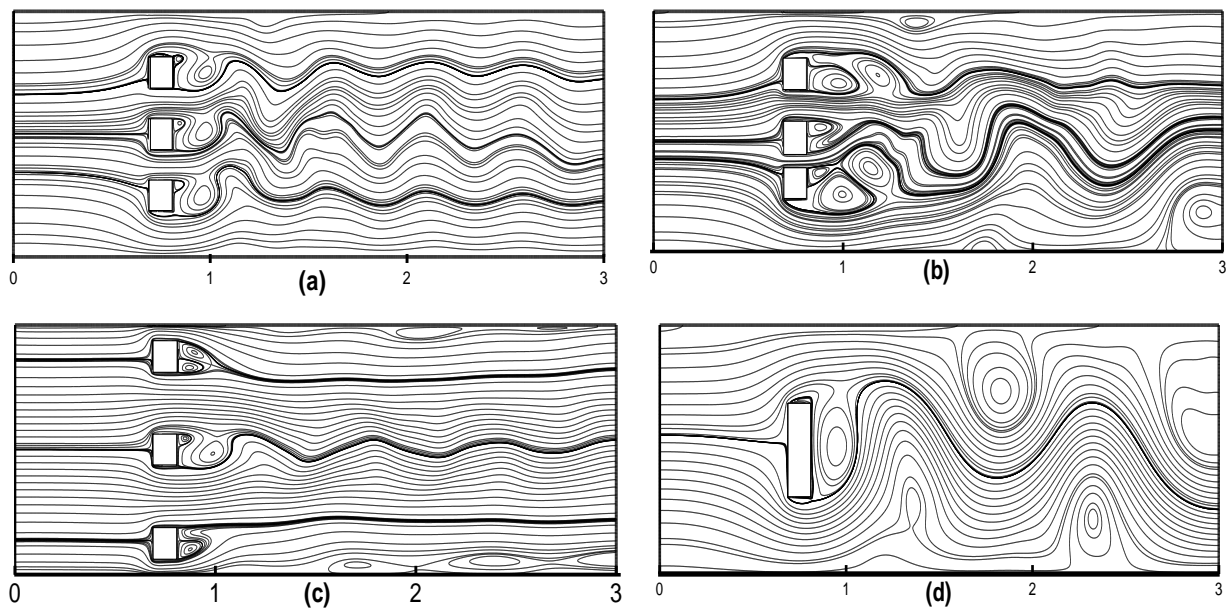


Fig. 9. Streamlines around square obstacles for different separation distances by setting the Reynolds number to 100.

For the isotherms, we see corrugations and recirculations distributed in a quasiperiodic and / or chaotic manner. In cases where $a_1 = a_2$, the vortices merge in the first case fig (a) after all the obstacles while they move in the second case (c). However, the regime keeps its symmetry. On the other hand, we observed that the vortices meet chaotically with each other just downstream of the obstacles fig (b, d).

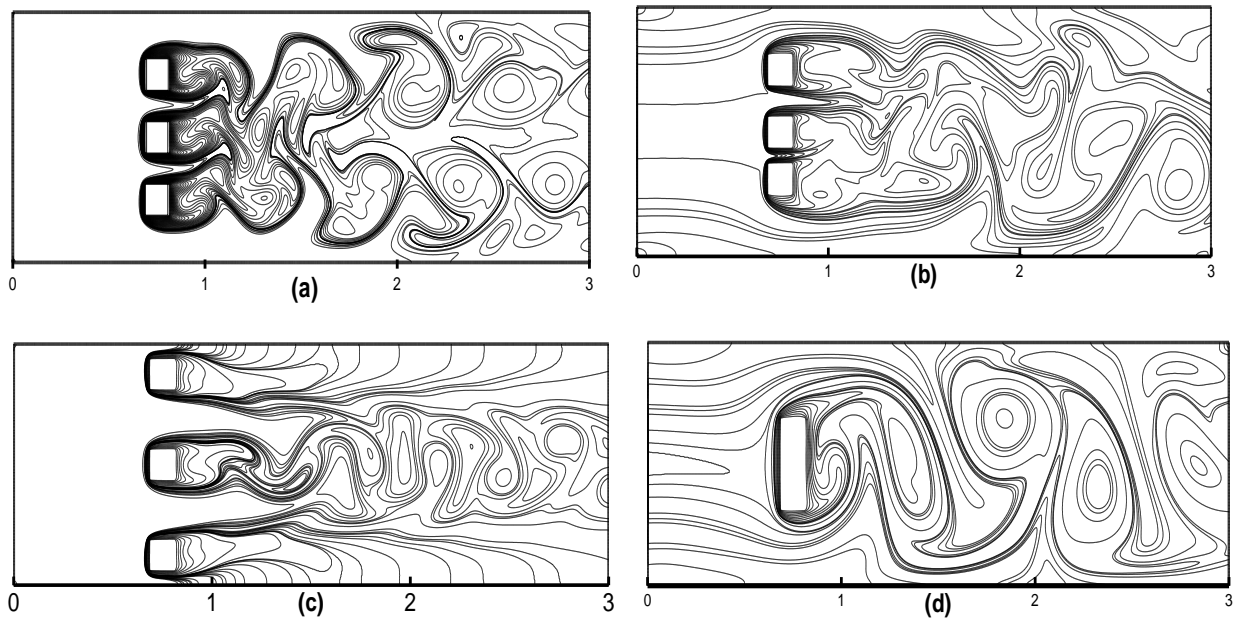


Fig. 10. Streamlines around square obstacles for different separation distances by setting the Reynolds number to 100.

Conclusion:

In this investigation, the effect of Re on a flow around three obstacles as well as the effect of spacing between these obstacles are explored using the lattice Boltzmann method. Flow tests around an isolated square obstacle are discussed to examine the sensitivity of the structure, domain sensitivity, and the code validation. The main results of this study show, firstly, that the Reynolds number has a significant effect on the flow structure. As Re increases, the regime changes from a stable and symmetrical state to an unstable and asymmetric state where vortex formation occurs, generating ripples along the flow. Similarly, the Reynolds number has a significant effect on the heat transfer; the isotherms are stable for low Re , while they are disturbed with increasing Re , which allows a maximum heat exchange. In addition, the distance separating the obstacles has a very important impact on the flow of the fluid. As can be seen, the decrease in this distance produces an increase in the amplitude of the vortices. Whereas if we change it, such as, either approaches the lower obstacle than the center one, or the opposite, there will be a remarkable fusion of vortex, which allows a maximum thermal transfer thanks to these vortices. Practically, this numerical work could lead to the prediction of the cooling of electronic components: The cooling of obstacles is all the better as the Reynolds number is important, and when these obstacles are the unequally spaced.

Nomenclature

a	constant parameter, $-4 < a < 1$
d/H	constriction ratio
f, g	density distribution function
f_{eq}, g_{eq}	equilibrium density distribution function
(g)	gap spacing between cylinders
H	channel width, m
L	channel length, m
l	block height, m
Pr	Prandtl number, $Pr = \nu/\alpha$

<i>Re</i>	<i>Reynolds number, $Re = U_{in} \cdot d/v$</i>
<i>SBS</i>	<i>side-by-side</i>
<i>T</i>	<i>dimensional temperature, K</i>
<i>u,v</i>	<i>x,y-velocity components, ms^{-1}</i>
<i>WSM</i>	<i>Wake-Scale Motions</i>

Greek symbols

α	<i>thermal diffusivity, m^2s^{-1}</i>
ρ	<i>density of fluid, $Kg.m^{-3}$</i>
θ	<i>dimensionless temperature, $\theta = (T - T_{in}) / (T_w - T_{in})$</i>
ν	<i>kinematic viscosity, m^2s^{-1}</i>

Subscripts

<i>in</i>	<i>inlet</i>
θ_c	<i>adimensional cold temperature</i>
θ_h	<i>adimensional hot temperature</i>
<i>w</i>	<i>wall</i>

Références

- [1] T.J. Young, K.Vafai, Convective cooling of a heated obstacle in a channel, *International Journal of Heat and Mass Transfer*, Vol.41, no 20, pp. 3131-3148,1998.
- [2] G. R. McNamara, G. Zanetti, Use of the Boltzmann equation to simulate lattice-gas automata, *Physical review letters*, Vol. 61, no 20, pp. 2332, 1988.
- [3] G. Nazeer. Numerical investigation of different flow regimes for multiple staggered rows. *AIP Advances*, Vol. 9, no 3, pp. 035247, 2019.
- [4] A. A. Alamyane, A. A. Mohamad, Simulation of forced convection in a channel with extended surfaces by the lattice Boltzmann method. *Computers & Mathematics with Applications*, Vol. 59, no 7, pp. 2421-2430, 2010.
- [5] M. A. Moussaoui, A. Mezrhab, and H. Naji, "A computation of flow and heat transfer past three heated cylinders in a vee shape by a double distribution MRT thermal lattice Boltzmann model," *International Journal of Thermal Sciences*. Vol. 50, pp.1532–1542, 2011.
- [6] A. Mezrhab, M.A. Moussaoui, M. Jami, H. Naji, M. Bouzidi, Double MRT thermal lattice Boltzmann method for simulating convective flows, *Physics Letters A*, Vol. 374, pp. 3499–3507, 2010.
- [7] M. Breuer, J. Bernsdorf, T. Zeiser, F. Durst, Accurate computations of the laminar flow past a square cylinder based on two different methods: lattice Boltzmann and finite-volume, *International Journal of Heat and Fluid Flow*, Vol. 21, no.2, pp.186-196, 2000.
- [8] M. M. Alam and Y. Zhou, "Intrinsic features of flow around two side-by side square cylinders," *Physics of Fluids*, Vol.25, pp. 085106-1–085106-21, 2013.
- [9] W. S. Abbasi, S. Ul. Islam, S. C. Saha, Y. T. Gu, and C. Y. Zhou, "Effect of Reynolds numbers on flow past four square cylinders in an in-line square configuration for different gap spacings," *Journal of Mechanical Science and Technology*, Vol. 28, pp. 539–552, 2014.
- [10] S. Ul. Islam, H. Rahman, C. Y. Zhou, and S. C. Saha, "Comparison of wake structures and force measurements behind three side-by-side cylinders," *Journal of the Brazilian Society of Mechanical Sciences and Engineering*, Vol. 38, pp. 843-858, 2016.

- [11] H. Rahman, S. Ul. Islam, C. Y. Zhou, T. Kiyani, and S. C. Saha, “On the effect of Reynolds number for flow past three side-by-side square cylinders for unequal gap spacings,” *KSCE Journal of Civil Engineering*, Vol. 19, pp. 233–247, 2015.
- [12] J. Mizushima and T. Akinaga, “Vortex shedding from a row of square bars,” *Fluid Dynamics Research*, Vol. 32, pp.179–191, 2003.
- [13] L. Djendi, “Lattice-Boltzmann simulation of grid-generated turbulence,” *Journal of Fluid Mechanics*, Vol. 552, pp. 13–35, 2006.
- [14] P. Le Gal, I. Peschard, M. P. Chauve, and Y. Takeda, “Collective behavior of wakes downstream of row of cylinders,” *Physics of Fluids*, Vol. 8, pp. 2097–2106, 1996.
- [15] S. Ul. Islam, H. Rahman, and C. Y. Zhou, “Effect of gap spacings on flow past row of rectangular cylinders with aspect ratio 1.5,” *Ocean Engineering*, Vol.119, pp. 1–15, 2016.
- [16] Moussaoui, M. A., Jami, M., Mezrhab, A., Naji, H., & Bouzidi, M. Multiple - relaxation time lattice Boltzmann computation of channel flow past a square cylinder with an upstream control bi - partition. *International Journal for Numerical Methods in Fluids*, Vol. 64, no 6, pp. 591-608, 2010.
- [17] d’Humières D. Generalized lattice Boltzmann equations. In *Rarefied Gas Dynamics: Theory and Simulations*, Shizgal BD, Weaver DP (eds). *Progress in Astronautics and Aeronautics*, vol. 159. AIAA Press: Washington, DC, pp. 450–458, 1992.
- [18] Bhatnagar PL, Gross EP, Krook M. A model for collision processes in gases. I. Small amplitude processes in charged and neutral one-component systems. *Physical Review Letters*, Vol.94, pp.511–525, 1954.
- [19] Lallemand P, Luo LS. Theory of the lattice Boltzmann method: dispersion, dissipation, isotropy, Galilean invariance, and stability. *Physical Review Letters E* 2000; 61:6546–6562.
- [20] D. d’Humières, *Progress in Astronautics and Aeronautics*, AIAA, Washington, DC, vol. 159, pp. 450, 1992.
- [21] A.A. Mohamad, *Lattice Boltzmann Method, Fundamentals and Engineering Application with Computer Codes*, Springer-Verlag, Landon, pp. 101–103, 2011.
- [22] M.A. Moussaoui, A computation of flow and heat transfer past three heated cylinders in a vee shape by a double distribution MRT thermal lattice Boltzmann model, *International Journal of Thermal Sciences*, pp.1532-1542, 2011.
- [23] C. Cercignani, *The Boltzmann Equation and Its Applications*. Applied Mathematical Sciences, Springer-Verlag, New York, Vol. 61, 1988.
- [24] M. Bouzidi, M. Firdaouss, P. Lallemand, Momentum transfer of a Boltzmann lattice fluid with boundaries, *Physics of Fluids*, Vol.13, no.11, pp. 3452-3459, 2001.
- [25] Q. Zou, X. He, on pressure and velocity boundary conditions for the lattice Boltzmann BGK model, *Physics of Fluids*, Vol.9, no.6, pp. 1591-1598, 1997
- [26] Davis, R.W., Moore, E.F., Purtell, L.P., A numerical-experimental study of confined Flow around rectangular cylinders, *Physics of Fluids*, Vol. 27 no.1, pp. 46–59, 1984.
- [27] Bernsdorf, J., Zeiser, T., Brenner, G., Durst, F., Simulation of 2D channel flow around a square obstacle with lattice-Boltzmann (BGK) automata. In: *Proceedings of the Seventh International Conference on the Discrete Simulation of Fluids*. University of Oxford, *International Journal of Modern Physics*, Vol. 9 no.8, pp.1129–1141, 14–18 July 1998.